Power Loading Algorithm for Orthogonalized Spatial Multiplexing in Wireless Communications

Young-Tae Kim*, Seokhwan Park* *Regular Members*, Inkyu Lee** *Lifelong Member*

ABSTRACT

In this paper, we propose a new power loading algorithm for orthogonalized spatial multiplexing (OSM) systems over flat-fading multiple-input multiple-output (MIMO) channels. Compared to SVD-based transmission scheme, the OSM scheme exhibits a good system performance with lower complexity and feedback overhead. To further improve the performance in OSM systems with power loading, we introduce a geometric approach on the Euclidean distance between the constellation points in the effective channel. Using this approach, we show that the optimal power loading parameters in terms of the minimum distance can be obtained. Simulation results demonstrate that our algorithm provides a 5dB gain at a bit error rate (BER) of 10^{-4} over that of no power loading case with both QPSK and 16-QAM. Consequently, our power loading algorithm allows us to significantly improve the system performance with one additional feedback value.

Key Words : MIMO; Closed loop; power allocation; maximizing dmin.

I. Introduction

Communication over multiple-input multiple-output (MIMO) channels has been the subject of intense research over the past several years, because the MIMO channel can offer much greater diversity gain and higher spatial multiplexing gain over their single-input single-output (SISO) counterpart[1][2][3]. Normally, two approaches have been considered to exploit many advantages of the MIMO channels. One is space-time coding that aims at maximizing diversity gain[4][5][6], and the other is spatial multiplexing which focuses on increasing the channel throughput[7][8][9].

If the communication environment is slowly time varying, the availability of channel state information (CSI) at the transmitter is possible via feedback or the reciprocal principle when time division duplex (TDD) is used. Many studies on such closed-loop MIMO systems have been based on singular value decomposition (SVD) of the channel transfer matrix[10][11]. However a drawback of precoding systems with the SVD is that the SVD operation requires high computational complexity and feedback overhead[12]. To reduce the feedback amount, a transmitter with limited feedback information was studied to utilize the system resources more efficiently[13][14].

Recently, orthogonalized spatial multiplexing (OSM) has been proposed, which achieves orthogonality between transmitted symbols by applying phase rotation at the transmitter[15][16]. The OSM scheme can be applied to a system with more than two transmit antennas, which transmits two streams of data at the same time. Compared to SVD-based transmission scheme, the OSM scheme exhibits a good system performance with lower complexity and feedback overhead.

One of salient features of the OSM scheme, is that transmitted data symbols experience the same

※ 본 연구는 지식경제부 및 정보통신연구진흥원의 대학 IT 연구센터 지원사업의 연구결과로 수행되었음(IITA-2008-C1090-0801-0013)
* 고려대학교 전자전기공학과 무선통신 연구실(reftm@korea.ac.kr)(shpark@wireless.korea.ac.kr)
** 고려대학교 전기전자전파공학부 무선통신 연구실(inkyu@korea.ac.kr)
논문번호 : KICS2008-12-532, 접수일자 : 2008년 12월 1일, 최종논문접수일자 : 2009년 4월 15일

channel quality. This may lead to an incorrect conclusion that the power loading would not improve the OSM performance. However, this is not the case since each component of the transmitted symbol still has different channel gains. Recognizing this issue, we propose a power loading scheme for OSM systems, which allocates the optimal power to each component instead of symbols. The proposed scheme requires one additional feedback value. To determine the optimal power level, we consider a criterion based on the Euclidean distance between the constellation points in the effective channel, since the minimum Euclidean distance accounts for the symbol error probability. We achieve reasonable receiver complexity from the proposed geometric approach. In the simulation section, we compare the performance of the proposed power loading for OSM systems with that of conventional OSM systems. The results show that our algorithm obtains a 5dB gain over no power loading case at a bit error rate (BER) of 10^{-4} with both QPSK and 16-QAM. Optimality of our proposed solution is confirmed by comparing with the exhaustive search results.

The remainder of this paper is organized as follows: Section Ⅱ presents the system model and reviews the OSM system. In Section Ⅲ, we propose a new power loading algorithm for OSM systems and a geometric approach for the criterion. In Section Ⅳ, simulation results are presented comparing the proposed scheme with OSM systems without power loading. Section Ⅴ gives the conclusions of this paper.

Ⅱ. System Descriptions

In this section, we consider a spatial multiplexing (SM) system with M_t transmit and M_r receive antennas in a frequency flat fading channel. Throughout this paper, normal letters represent scalar quantities, boldface letters indicate vectors and boldface uppercase letters designate matrices. With a bar accounting for complex variables, for any complex notation $\bar{c}$, we denote the real and imaginary part of $\bar{c}$ by $R[\bar{c}]$ and $I[\bar{c}]$, respectively.

We consider the complex channel output as

$$\bar{\mathbf{y}} = \bar{\mathbf{H}}\bar{\mathbf{x}} + \bar{\mathbf{n}} \tag{1}$$

where $\bar{\mathbf{x}} \in \mathbf{C}^{M_t \times 1}$ is the complex transmitted signal, $\bar{\mathbf{y}} \in \mathbf{C}^{M_r \times 1}$ indicates the complex received signal, and $\bar{\mathbf{H}} \in \mathbf{C}^{M_r \times M_t}$ represents the complex channel matrix with the (i,j)th element denoting the fading coefficient between the jth transmit and the ith receive antenna. We assume that the elements of the MIMO channel matrix $\bar{\mathbf{H}}$ are obtained from an independent and identically distributed (i.i.d) complex Gaussian distribution. Each channel realization is assumed to be known at the receiver. Also, we assume that $\bar{\mathbf{n}} \sim N(0, \sigma_n^2 \mathbf{I}_{M_r})$ is the zero-mean circularly symmetric complex Gaussian noise, where $\mathbf{I}_{M_r}$ denotes an identity matrix of size M_r.

In what follows, we give a brief review on the orthogonalized spatial multiplexing (OSM) scheme in [15][16]. We focus on a system transmitting two independent data streams. The OSM orthogonalizes a channel by applying a rotation precoder. Thus the joint ML detector reduces to a single symbol decodable receiver, which greatly decreases the detection complexity.

To orthogonalize the channel, the OSM precodes two transmitted symbols as

$$F(\bar{\mathbf{x}}, \theta) = \begin{bmatrix} 1 & 0 \\ 0 & \exp(j\theta) \end{bmatrix} \mathbf{s}(\bar{\mathbf{x}})$$

where θ is the rotation phase angle applied to the second antenna and

$$\mathbf{s}(\bar{\mathbf{x}}) = \begin{bmatrix} R[\bar{x_1}] + jR[\bar{x_2}] \\ I[\bar{x_1}] + jI[\bar{x_2}] \end{bmatrix} = \begin{bmatrix} s_1(\bar{x}) \\ s_2(\bar{x}) \end{bmatrix}.$$

Employing the above precoding, equation (1) can be rewritten as

$$\bar{\mathbf{y}} = \bar{\mathbf{H}} F(\bar{\mathbf{x}}, \theta) + \bar{\mathbf{n}} = \bar{\mathbf{H}}_\theta \mathbf{s}(\bar{\mathbf{x}}) + \bar{\mathbf{n}} \tag{2}$$

where $\overline{\mathbf{H}}_\theta$ accounts for the effective channel matrix for $\mathbf{s}(\overline{\mathbf{x}})$, represented by

$$\overline{\mathbf{H}}_\theta = \overline{\mathbf{H}} \begin{bmatrix} 1 & 0 \\ 0 & \exp(j\theta) \end{bmatrix}.$$

Equivalently, the real-valued representation of the system (2) is given as [15][16]

$$\begin{aligned} \mathbf{y} &= \mathbf{H}_\theta \mathbf{s}(\mathbf{x}) + \mathbf{n} \\ &= \begin{bmatrix} R[\overline{\mathbf{y}}] \\ I[\overline{\mathbf{y}}] \end{bmatrix} = \begin{bmatrix} R[\overline{\mathbf{H}_\theta}] & -I[\overline{\mathbf{H}_\theta}] \\ I[\overline{\mathbf{H}_\theta}] & R[\overline{\mathbf{H}_\theta}] \end{bmatrix} \begin{bmatrix} R[\mathbf{s}(\overline{\mathbf{x}})] \\ I[\mathbf{s}(\overline{\mathbf{x}})] \end{bmatrix} + \begin{bmatrix} R[\overline{\mathbf{n}}] \\ I[\overline{\mathbf{n}}] \end{bmatrix} \\ &= [\, \mathbf{h}_1^\theta \ \mathbf{h}_2^\theta \ \mathbf{h}_3^\theta \ \mathbf{h}_4^\theta \,] \mathbf{s}(\mathbf{x}) + \mathbf{n} \end{aligned} \quad (3)$$

where the real column vector $\mathbf{h}_i^\theta$ of length $2M_r$ denotes the ith column of the effective real-valued channel matrix $\mathbf{H}_\theta$, $\mathbf{s}(\mathbf{x})$ represents $[R[\overline{x}_1]\, I[\overline{x}_1]\, R[\overline{x}_2]\, I[\overline{x}_2]]$ and $\mathbf{n}$ indicates $[R[\overline{\mathbf{n}}^T]\, I[\overline{\mathbf{n}}^T]]^T$.

From the real-valued representation of the channel matrix in (3), it is easy to see that the column vectors $\mathbf{h}_1^\theta$ and $\mathbf{h}_2^\theta$ are orthogonal to $\mathbf{h}_3^\theta$ and $\mathbf{h}_4^\theta$, respectively ($\mathbf{h}_1^\theta \perp \mathbf{h}_3^\theta$ and $\mathbf{h}_2^\theta \perp \mathbf{h}_4^\theta$), regardless of θ. We also notice that $\mathbf{h}_1^\theta \cdot \mathbf{h}_4^\theta = -\mathbf{h}_2^\theta \cdot \mathbf{h}_3^\theta$ for all θ, where $\mathbf{a} \cdot \mathbf{b}$ denotes the inner (dot) product between vectors a and b. In this case, $\mathbf{H}_\theta$ becomes orthogonal if and only if $\mathbf{h}_1^\theta \perp \mathbf{h}_4^\theta$ and $\mathbf{h}_2^\theta \perp \mathbf{h}_3^\theta$ ($\mathbf{h}_1^\theta \cdot \mathbf{h}_4^\theta = -\mathbf{h}_2^\theta \cdot \mathbf{h}_3^\theta = 0$).

Denoting $\overline{h}_{ij}$ as the (i,j)th entry of $\overline{\mathbf{H}}$, the rotation angle for the orthogonality between $\mathbf{h}_1^\theta$ and $\mathbf{h}_4^\theta$ (or $\mathbf{h}_2^\theta$ and $\mathbf{h}_3^\theta$) can be written as[15][16]

$$\theta = \tan^{-1}\left(\frac{B}{A}\right) \pm \frac{\pi}{2}$$

where $A = \sum_{m=1}^{M_r} |\overline{h}_{m1}||\overline{h}_{m2}| \sin(\angle \overline{h}_{m2} - \angle \overline{h}_{m1})$ and $B = \sum_{m=1}^{M_r} |\overline{h_{m1}}||\overline{h_{m2}}| \cos(\angle \overline{h_{m2}} - \angle \overline{h_{m1}})$. This rotation angle makes symbols orthogonal to each other.

Utilizing this orthogonality, the ML estimate of transmitted symbol $\hat{\overline{x}}_1$ and $\hat{\overline{x}}_2$ can be obtained as[15][16]

$$\hat{\overline{x}}_1 = \arg\min_{\overline{x}_1 \in Q} \left\| \mathbf{y} - [\mathbf{h}_1^\theta \mathbf{h}_2^\theta] \begin{bmatrix} R[\overline{x}_1] \\ I[\overline{x}_1] \end{bmatrix} \right\|^2 \quad (4)$$

and

$$\hat{\overline{x}}_2 = \arg\min_{\overline{x}_2 \in Q} \left\| \mathbf{y} - [\mathbf{h}_3^\theta \mathbf{h}_4^\theta] \begin{bmatrix} R[\overline{x}_2] \\ I[\overline{x}_2] \end{bmatrix} \right\|^2 \quad (5)$$

where Q is a signal constellation of size M_c.

As a result, the complexity of the ML estimation of the OSM reduces from M_c^2 to M_c. Compared to SVD-based transmission schemes, the OSM has lower complexity and feedback overhead[15][16].

Ⅲ. Power Loading Algorithm for OSM

First we discuss about the necessity of power loading for OSM systems. From equations (4) and (5), a solution for an OSM system is transformed into two single-input single-output (SISO) systems. In general, componentwise power loading for SISO systems does not improve the system performance, since real and imaginary parts of a transmitted symbol have the same channel gain and are orthogonal to each other. However the SISO equations (4) and (5) is different from the conventional SISO systems.

Note that $\mathbf{h}_1^\theta$, $\mathbf{h}_2^\theta$, $\mathbf{h}_3^\theta$ and $\mathbf{h}_4^\theta$ are the channel gains of the components within two transmitted symbols. It was shown in [15][16] that the subspace spanned by $\mathbf{h}_1^\theta$ and $\mathbf{h}_2^\theta$ is orthogonal to that spanned by $\mathbf{h}_3^\theta$ and $\mathbf{h}_4^\theta$ with the OSM precoding. It is easy to see that $\|\mathbf{h}_1^\theta\| = \|\mathbf{h}_3^\theta\|$, $\|\mathbf{h}_2^\theta\| = \|\mathbf{h}_4^\theta\|$ and $\mathbf{h}_1^\theta \cdot \mathbf{h}_2^\theta = \mathbf{h}_3^\theta \cdot \mathbf{h}_4^\theta$. From this observation, it appears that power loading is not necessary for the OSM scheme. However the column vectors $\mathbf{h}_1^\theta$ and $\mathbf{h}_3^\theta$ are not orthogonal to $\mathbf{h}_2^\theta$ and $\mathbf{h}_4^\theta$, respectively. Also, $\|\mathbf{h}_1^\theta\| = \|\mathbf{h}_3^\theta\|$ is not equal to $\|\mathbf{h}_2^\theta\| = \|\mathbf{h}_4^\theta\|$. As a result, the channel energy corresponding to the inphase and quadrature components is still different.

Motivated by this observation, we present a componentwise power loading algorithm for OSM systems. For the optimum ML receiver, performance depends on the minimum Euclidean distance in the received signal constellation, denoted by $d_{\min}$ [17]. Thus, we focus on maximizing $d_{\min}$ by means of a geometric approach.

Define the power loading matrix and the power loading parameter as P and p, respectively. We also denote $\sqrt{2-p^2}$ as $\bar{p}$. We assume that the total transmit power is constrained to be $\mathrm{E}[\mathrm{tr}(\mathbf{Ps}(\mathbf{x})\mathbf{s}(\mathbf{x})^{\mathrm{T}}\mathbf{P}^{\mathrm{T}})]=P_T$ which equals to $\mathrm{tr}(\mathbf{PP}^{\mathrm{T}})=4$ if $\mathrm{E}[\mathrm{tr}(\mathbf{s}(\mathbf{x})\mathbf{s}(\mathbf{x})^{\mathrm{T}})]=P_T$. Then, the received signal in (3) can be rewritten as

$$\mathbf{y}=\mathbf{H}_\theta\mathbf{Ps}(\mathbf{x})+\mathbf{n}$$

where $\mathbf{P}=\mathrm{diag}\{p,\bar{p},p,\bar{p}\}$. Fig. 1 depicts the structure of the power allocation for OSM systems.

Let us denote the first and second column vector of $\mathbf{H}_\theta\mathbf{P}$ as $\mathbf{h}_{1p}^{\theta}=p\mathbf{h}_1^{\theta}$ and $\mathbf{h}_{2\bar{p}}^{\theta}=\bar{p}\mathbf{h}_2^{\theta}$, respectively. Since two SISO equations (4) and (5) have the same expression within one OSM system, our analysis is carried out on only one SISO equation. From now on, we refer to $[\mathbf{h}_{1p}^{\theta},\mathbf{h}_{2\bar{p}}^{\theta}]$ as the effective channel matrix with power loading. Then ML equation (4) can be rewritten as

$$\hat{\bar{x}}_1=\arg\min_{\bar{x}_1\in Q}\left\|\mathbf{y}-\left[\mathbf{h}_{1p}^{\theta}\,\mathbf{h}_{2\bar{p}}^{\theta}\right]\begin{bmatrix}R[\bar{x}_1]\\ I[\bar{x}_1]\end{bmatrix}\right\|^2 \quad (6)$$

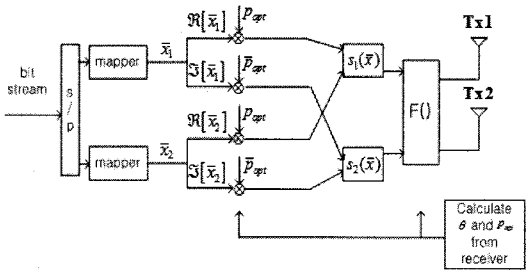

그림 1. OSM을 위한 전력 할당 시스템 구조도
Fig. 1. Schematic diagram of transmitter structure for OSM systems with power loading

To maximize $d_{\min}$, we present a power loading algorithm with the following criteria

$$p_{opt}=\arg\max_{0\le p\le\sqrt{2}}d_{\min}(p). \quad (7)$$

where $d_{\min}(p)$ is the minimum distance as p. The optimal power loading parameter p_{opt} in (7) is dependent on modulation levels. For the remainder of this section, we present the analysis results on QPSK and 16-QAM constellations. We first start with a theorem to introduce a geometric analysis.

Theorem 3.1 : Let $n>0$ be an arbitrary integer number. We assume a triangle with side lengths t, nt and t'. Assuming that θ_t, θ_{nt} and $\theta_{t'}$ represent the opposite angle of t, nt and t', respectively, where θ_t is an acute angle, we have $\theta_t\le\sin^{-1}(1/n)$.

proof : Denote R as the radius of a circumcircle of the above triangle. Then, we have $2R\sin(\theta_{nt})=nt$ and $2R\sin(\theta_t)=t$. Since $2R\sin(\theta_{nt})/2R\sin(\theta_t)=t$, it follows

$$\theta_t=\sin^{-1}\{(1/n)\sin(\theta_{nt})\}\le\sin^{-1}(1/n).$$

For QPSK constellations, we assume that the real or imaginary part of the transmitted symbol has its value $\pm1/2$. From the ML equation (6), the constellations points in the effective channel are $\left(\mathbf{h}_{1p}^{\theta}+\mathbf{h}_{2\bar{p}}^{\theta}\right)/2$, $\left(-\mathbf{h}_{1p}^{\theta}+\mathbf{h}_{2\bar{p}}^{\theta}\right)/2$, $\left(-\mathbf{h}_{1p}^{\theta}-\mathbf{h}_{2\bar{p}}^{\theta}\right)/2$ and $\left(\mathbf{h}_{1p}^{\theta}-\mathbf{h}_{2\bar{p}}^{\theta}\right)/2$. Then, the criteria of (7) can be rewritten as

$$p_{opt}=\arg\max_{0\le p\le\sqrt{2}}[\min(\|\mathbf{h}_{1p}^{\theta}\|,\ \|\mathbf{h}_{2\bar{p}}^{\theta}\|,\|\mathbf{h}_{1p}^{\theta}+\mathbf{h}_{2\bar{p}}^{\theta}\|,\|\mathbf{h}_{1p}^{\theta}-\mathbf{h}_{2\bar{p}}^{\theta}\|)]. \quad (8)$$

In what follows, we present an efficient way to determine p_{opt} which guarantees a better performance by maximizing $d_{\min}$ based on the geometric approach. Define the angle between $\mathbf{h}_1^{\theta}$ and $\mathbf{h}_2^{\theta}$ as θ_c.. If θ_c is an acute angle, $\|\mathbf{h}_{1p}^{\theta}+\mathbf{h}_{2\bar{p}}^{\theta}\|$ cannot be minimum. Thus

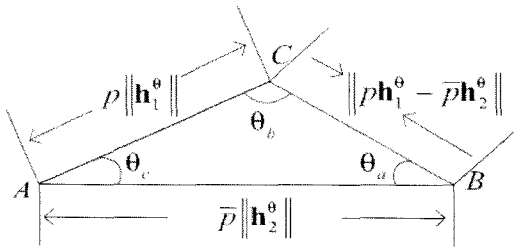

그림 2. QPSK에서의 $d_{\min}$ 접근을 위한 삼각형 모델
Fig. 2. Triangle model for geometric approach on $d_{\min}$ for QPSK

$\|\mathbf{h}_{1p}^\theta + \mathbf{h}_{2\bar{p}}^\theta\|$ can be neglected in (8). Each side of triangle ABC in Fig. 2 shows the candidate for $d_{\min}$. Since the analysis for acute angles and obtuse angles is symmetric, we only consider the case of an acute angle in this paper. By changing θ_c with $(180^\circ - \theta_c)$, the obtuse angle case yields the same result.

For the analysis of QPSK, θ_c is classified into the following two cases.

1) $60^\circ \le \theta_c \le 90^\circ \; (0 \le \cos\theta_c \le 0.5)$

We first show that $\|\mathbf{h}_{1p}^\theta - \mathbf{h}_{2\bar{p}}^\theta\|$ can never be the shortest side of the triangle ABC. If we assume that $\|\mathbf{h}_{1p}^\theta - \mathbf{h}_{2\bar{p}}^\theta\|$ is the shortest side, θ_c should be the smallest angle inside the triangle. This means that θ_a and θ_b are larger than θ_c ($\theta_a > \theta_c \ge 60^\circ$, $\theta_b > \theta_c \ge 60^\circ$), which contradicts the triangle.

From this observation, we can simplify the problem as $d_{\min}(p) = \min(\|\mathbf{h}_{1p}^\theta\|, \|\mathbf{h}_{2\bar{p}}^\theta\|)$. As can be guessed from Fig. 2, this equation can be rewritten as

$$d_{\min}(p) = \begin{cases} \|\mathbf{h}_{1p}^\theta\| & \text{if } 0 < p \le k_1 \\ \|\mathbf{h}_{2\bar{p}}^\theta\| & \text{if } k_1 < p < \sqrt{2} \end{cases}$$

where k_1 is obtained as $\|\mathbf{h}_{1p}^\theta\| = \|\mathbf{h}_{2\bar{p}}^\theta\|$ for $p = k_1$. Since $\|\mathbf{h}_{1p}^\theta\|$ is a monotonically increasing function of p and $\|\mathbf{h}_{2\bar{p}}^\theta\|$ is a monotonically decreasing function of p, we have $\arg\max_p(d_{\min}) = k_1$. The closed form solution for k_1 is given in case 1 in Appendix A.

2) $0^\circ \le \theta_c < 60^\circ \; (0.5 \le \cos\theta_c \le 1)$

It can be shown in Fig. 2 that $d_{\min}$ can be obtained as

$$d_{\min}(p) = \begin{cases} \|\mathbf{h}_{1p}^\theta\| & \text{if } 0 < p \le k_2 \\ \|\mathbf{h}_{1p}^\theta - \mathbf{h}_{2\bar{p}}^\theta\| & \text{if } k_2 < p \le k_3 \\ \|\mathbf{h}_{2\bar{p}}^\theta\| & \text{if } k_3 < p < \sqrt{2} \end{cases} \quad (9)$$

where k_2 and k_3 are defined as $\|\mathbf{h}_{1p}^\theta\| = \|\mathbf{h}_{1p}^\theta - \mathbf{h}_{2\bar{p}}^\theta\|$ for $p = k_2$ and $\|\mathbf{h}_{2\bar{p}}^\theta\| = \|\mathbf{h}_{1p}^\theta - \mathbf{h}_{2\bar{p}}^\theta\|$ for $p = k_3$.

By taking the second derivative of $\|\mathbf{h}_{1p}^\theta - \mathbf{h}_{2\bar{p}}^\theta\|^2$ in terms of p, we can verify that $\|\mathbf{h}_{1p}^\theta - \mathbf{h}_{2\bar{p}}^\theta\|$ is a convex-down function of p. Also $\|\mathbf{h}_{1p}^\theta\|$ is a monotonically increasing function of p and $\|\mathbf{h}_{2\bar{p}}^\theta\|$ is a monotonically decreasing function of p. From the preceding description and the criteria (7), the optimum power loading parameter p_{opt} can be either k_2 or k_3, where k_2 and k_3 can be obtained from case 2 and case 3 in the Appendix, respectively. Inserting k_2 and k_3 obtained from the Appendix into (9) yields

$$d_{\min}(p) = \begin{cases} \sqrt{\dfrac{2\|\mathbf{h}_2^\theta\|^2}{4\cos^2\theta + \|\mathbf{h}_2^\theta\|^2/\|\mathbf{h}_1^\theta\|^2}} & \text{if } p = k_2 \\ \sqrt{\dfrac{2\|\mathbf{h}_1^\theta\|^2}{4\cos^2\theta + \|\mathbf{h}_1^\theta\|^2/\|\mathbf{h}_2^\theta\|^2}} & \text{if } p = k_3. \end{cases}$$

From the above equation, we can compute p_{opt} as

$$p_{opt} = \begin{cases} k_2 & \text{if } \|\mathbf{h}_1^\theta\| < \|\mathbf{h}_2^\theta\| \\ k_3 & \text{if } \|\mathbf{h}_2^\theta\| < \|\mathbf{h}_1^\theta\|. \end{cases}$$

Note that we do not need to calculate both k_2 and k_3.

Next, we consider the 16-QAM case. For 16-QAM constellations, we assume that the real or imaginary part of the transmitted symbol has its value $\pm 1/2, \pm 3/2$. Then, the candidates of $d_{\min}$ are as follows: $\|\mathbf{h}_{1p}^\theta\|$, $\|\mathbf{h}_{2\bar{p}}^\theta\|$,

$\| \mathbf{h}_{1p}^{\theta} - \mathbf{h}_{2\bar{p}}^{\theta} \|$, $\| \mathbf{h}_{1p}^{\theta} + \mathbf{h}_{2\bar{p}}^{\theta} \|$, $\| \mathbf{h}_{1p}^{\theta} - 2\mathbf{h}_{2\bar{p}}^{\theta} \|$, $\| \mathbf{h}_{1p}^{\theta} + 2\mathbf{h}_{2\bar{p}}^{\theta} \|$, $\| 2\mathbf{h}_{1p}^{\theta} - \mathbf{h}_{2\bar{p}}^{\theta} \|$, $\| 2\mathbf{h}_{1p}^{\theta} + \mathbf{h}_{2\bar{p}}^{\theta} \|$, $\| \mathbf{h}_{1p}^{\theta} - 3\mathbf{h}_{2\bar{p}}^{\theta} \|$, $\| \mathbf{h}_{1p}^{\theta} + 3\mathbf{h}_{2\bar{p}}^{\theta} \|$, $\| 3\mathbf{h}_{1p}^{\theta} - \mathbf{h}_{2\bar{p}}^{\theta} \|$, $\| 3\mathbf{h}_{1p}^{\theta} + \mathbf{h}_{2\bar{p}}^{\theta} \|$, $\| 3\mathbf{h}_{1p}^{\theta} - 2\mathbf{h}_{2\bar{p}}^{\theta} \|$, $\| 3\mathbf{h}_{1p}^{\theta} + 2\mathbf{h}_{2\bar{p}}^{\theta} \|$, $\| 2\mathbf{h}_{1p}^{\theta} - 3\mathbf{h}_{2\bar{p}}^{\theta} \|$, $\| 2\mathbf{h}_{1p}^{\theta} + 3\mathbf{h}_{2\bar{p}}^{\theta} \|$. Similar to QPSK, we only analyze the case of an acute angle. In this assumption, $\| \mathbf{h}_{1p}^{\theta} \|$ is smaller than $\| \mathbf{h}_{1p}^{\theta} + \mathbf{h}_{2\bar{p}}^{\theta} \|$, $\| \mathbf{h}_{1p}^{\theta} + 2\mathbf{h}_{2\bar{p}}^{\theta} \|$, $\| 2\mathbf{h}_{1p}^{\theta} + \mathbf{h}_{2\bar{p}}^{\theta} \|$, $\| \mathbf{h}_{1p}^{\theta} + 3\mathbf{h}_{2\bar{p}}^{\theta} \|$, $\| 3\mathbf{h}_{1p}^{\theta} + \mathbf{h}_{2\bar{p}}^{\theta} \|$, $\| 3\mathbf{h}_{1p}^{\theta} + 2\mathbf{h}_{2\bar{p}}^{\theta} \|$ or $\| 2\mathbf{h}_{1p}^{\theta} + 3\mathbf{h}_{2\bar{p}}^{\theta} \|$, regardless of p.

We analyze the case of $\| \mathbf{h}_1^{\theta} \| \le \| \mathbf{h}_2^{\theta} \|$ only, since the solution for $\| \mathbf{h}_1^{\theta} \| > \| \mathbf{h}_2^{\theta} \|$ can be obtained symmetrically. From the QPSK analysis, we can notice that if $\| \mathbf{h}_1^{\theta} \| \le \| \mathbf{h}_2^{\theta} \|$, we have $\| \mathbf{h}_{1p}^{\theta} \| \le \| \mathbf{h}_{2\bar{p}}^{\theta} \|$ for $p = p_{opt}$, and vice versa. In other words, the inequality between $\| \mathbf{h}_1^{\theta} \|$ and $\| \mathbf{h}_2^{\theta} \|$ remains unchanged after the optimal power loading. Then, the following inequalities hold:

$\| \mathbf{h}_{1p}^{\theta} \| \le \| \mathbf{h}_{2\bar{p}}^{\theta} \|$,

$\| 2\mathbf{h}_{1p}^{\theta} - \mathbf{h}_{2\bar{p}}^{\theta} \| \le \| \mathbf{h}_{1p}^{\theta} - 2\mathbf{h}_{2\bar{p}}^{\theta} \|$,

$\| 3\mathbf{h}_{1p}^{\theta} - \mathbf{h}_{2\bar{p}}^{\theta} \| \le \| \mathbf{h}_{1p}^{\theta} - 3\mathbf{h}_{2\bar{p}}^{\theta} \|$,

$\| 3\mathbf{h}_{1p}^{\theta} - 2\mathbf{h}_{2\bar{p}}^{\theta} \| \le \| 2\mathbf{h}_{1p}^{\theta} - 3\mathbf{h}_{2\bar{p}}^{\theta} \|$ for $p = p_{opt}$.

Consequently, we have the search candidates for computing $d_{\min}$ as

$$p_{opt} = \arg\max_{0 \le p \le \sqrt{2}} [\min(\| \mathbf{h}_{1p}^{\theta} \|, \| \mathbf{h}_{1p}^{\theta} - \mathbf{h}_{2\bar{p}}^{\theta} \|, \| 2\mathbf{h}_{1p}^{\theta} - \mathbf{h}_{2\bar{p}}^{\theta} \|, \| 3\mathbf{h}_{1p}^{\theta} - \mathbf{h}_{2\bar{p}}^{\theta} \|)]. \quad (10)$$

where lines $\overline{AC}$, $\overline{BC}$, $\overline{BD}$ and $\overline{BE}$ in Fig. 3, which correspond to each candidate. Since simulation results show that $\| 3\mathbf{h}_{1p}^{\theta} - 2\mathbf{h}_{2\bar{p}}^{\theta} \|$ is not critical, we will not consider $\| 3\mathbf{h}_{1p}^{\theta} - 2\mathbf{h}_{2\bar{p}}^{\theta} \|$.

For the analysis of 16-QAM, θ_c is classified into the following three cases.

1) $30^\circ \le \theta_c \le 90^\circ$ $(0 \le \cos\theta_c \le 0.8661)$

For this range of θ_c, from Theorem 3.1, the length of $\overline{AD}$ cannot be twice the length of $\overline{BD}$ in the triangle ABC. Note that the lengths of $\overline{AC}$ and $\overline{BD}$ are continuous functions of p. Using these results, we notice that length of $\overline{AC}$ cannot be equal that of $\overline{BD}$. Since the above statement holds for all possible p, we can simply check the case of $p = 0$ which results in $\| 2\mathbf{h}_{1p}^{\theta} - \mathbf{h}_{2\bar{p}}^{\theta} \| \le \| \mathbf{h}_{1p}^{\theta} \|$. Thus, we conclude that $\| 2\mathbf{h}_{1p}^{\theta} - \mathbf{h}_{2\bar{p}}^{\theta} \|$ is always greater than $\| \mathbf{h}_{1p}^{\theta} \|$ for all possible p. Similar to this, $\| 3\mathbf{h}_{1p}^{\theta} - \mathbf{h}_{2\bar{p}}^{\theta} \|$ is always greater than $\| \mathbf{h}_{1p}^{\theta} \|$ for all possible p. As a result, we only need to compare $\| \mathbf{h}_{1p}^{\theta} \|$ and $\| \mathbf{h}_{1p}^{\theta} - \mathbf{h}_{2\bar{p}}^{\theta} \|$ in (10). Since the candidates $\| \mathbf{h}_{1p}^{\theta} \|$ and $\| \mathbf{h}_{1p}^{\theta} - \mathbf{h}_{2\bar{p}}^{\theta} \|$ are the same as the QPSK case for $\| \mathbf{h}_{1p}^{\theta} \| \le \| \mathbf{h}_{2\bar{p}}^{\theta} \|$, we omit the analysis.

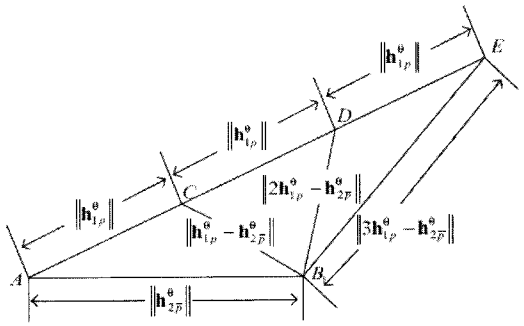

그림 3. 16QAM에서 $d_{\min}$ 접근을 위한 삼각형 모델
Fig. 3. Triangle model for geometric approach on $d_{\min}$ for 16QAM

2) $19.47^\circ \le \theta_c < 30^\circ$ $(0.866 < \cos\theta_c \le 0.943)$

Similar to the above case, $\| 3\mathbf{h}_{1p}^{\theta} - \mathbf{h}_{2\bar{p}}^{\theta} \|$ are greater than $\| \mathbf{h}_{1p}^{\theta} \|$, regardless of p. Thus, the candidates of $d_{\min}$ in (10) reduce to $\| \mathbf{h}_{1p}^{\theta} \|$, $\| \mathbf{h}_{1p}^{\theta} - \mathbf{h}_{2\bar{p}}^{\theta} \|$ and $\| 2\mathbf{h}_{1p}^{\theta} - \mathbf{h}_{2\bar{p}}^{\theta} \|$. By examining Fig. 3, $d_{\min}$ can be written as

$$d_{\min}(p) = \begin{cases} \| \mathbf{h}_{1p}^{\theta} \| & \text{if } 0 < p \le k_4 \\ \| 2\mathbf{h}_{1p}^{\theta} - \mathbf{h}_{2\bar{p}}^{\theta} \| & \text{if } k_4 < p \le k_5 \\ \| \mathbf{h}_{1p}^{\theta} - \mathbf{h}_{2\bar{p}}^{\theta} \| & \text{if } k_5 < p \le k_1 \end{cases}$$

where k_4 and k_5 are obtained as

표 1. $\| \mathbf{h}_1^\theta \| \le \| \mathbf{h}_2^\theta \|$ 일 때 최적의 전력 할당 계수 p_{opt}
Table 1. Optimal Power Lodaing Parameter p_{opt} for $\| \mathbf{h}_1^\theta \| \le \| \mathbf{h}_2^\theta \|$

Mod	Case	p_{opt}
QPSK	$0 \le \lvert\cos\theta_c\rvert \le 0.5$	k_1
	$0.5 < \lvert\cos\theta_c\rvert \le 1$	k_2
16-QAM	$0 \le \lvert\cos\theta_c\rvert \le 0.5$	k_1
	$0.5 < \lvert\cos\theta_c\rvert \le 0.866$	k_2
	$0.866 < \lvert\cos\theta_c\rvert \le 0.9$	k_5 if $\| \mathbf{h}_1^\theta \| \le \| \mathbf{h}_2^\theta \| < 3 \| \mathbf{h}_1^\theta \|$ k_4 if $3 \| \mathbf{h}_1^\theta \| \le \| \mathbf{h}_2^\theta \|$
	$0.9 < \lvert\cos\theta_c\rvert \le 0.943$	k_5 if $\| \mathbf{h}_1^\theta \| \le \| \mathbf{h}_2^\theta \| < 2 \| \mathbf{h}_1^\theta \|$ k_4 if $2 \| \mathbf{h}_1^\theta \| \le \| \mathbf{h}_2^\theta \|$
	$0.943 < \lvert\cos\theta_c\rvert \le 0.966$	k_5 if $\| \mathbf{h}_1^\theta \| \le \| \mathbf{h}_2^\theta \| < 2 \| \mathbf{h}_1^\theta \|$ k_7 if $2 \| \mathbf{h}_1^\theta \| \le \| \mathbf{h}_2^\theta \| < 3 \| \mathbf{h}_1^\theta \|$ k_6 if $3 \| \mathbf{h}_1^\theta \| \le \| \mathbf{h}_2^\theta \|$
	$0.966 < \lvert\cos\theta_c\rvert \le 0.985$	k_5 if $\| \mathbf{h}_1^\theta \| \le \| \mathbf{h}_2^\theta \| < 2 \| \mathbf{h}_1^\theta \|$ k_6 if $2 \| \mathbf{h}_1^\theta \| \le \| \mathbf{h}_2^\theta \|$
	$0.985 < \lvert\cos\theta_c\rvert \le 1$	k_6

$\| \mathbf{h}_{1p}^\theta \| = \| 2\mathbf{h}_{1p}^\theta - \mathbf{h}_{2\bar{p}}^\theta \|$ for $p = k_4$ and $\| 2\mathbf{h}_{1p}^\theta - \mathbf{h}_{2\bar{p}}^\theta \| = \| \mathbf{h}_{1p}^\theta - \mathbf{h}_{2\bar{p}}^\theta \|$ for $p = k_5$. There are two solutions for $\| \mathbf{h}_{1p}^\theta \| = \| 2\mathbf{h}_{1p}^\theta - \mathbf{h}_{2\bar{p}}^\theta \|$. After analyzing the geometric relation, it can be shown that the smaller one should be chosen as k_4.

Since $\| \mathbf{h}_{1p}^\theta \|$ is a monotonically increasing function of p and $\| 2\mathbf{h}_{1p}^\theta - \mathbf{h}_{2\bar{p}}^\theta \|$, $\| \mathbf{h}_{1p}^\theta - \mathbf{h}_{2\bar{p}}^\theta \|$ are convex-down functions, p_{opt} is either k_4, k_5 or k_1, where k_4 and k_5 can be calculated from case 4 and case 3 in the Appendix, respectively. The condition on which value should be selected among k_4, k_5 and k_1 can be determined by analyzing the geometry, and the result is listed in Table 1.

3) $0^\circ \le \theta_c < 19.47^\circ \; (0.943 < \cos\theta_c \le 1)$

Similar to the analysis presented above, $d_{\min}$ is given as

$$d_{\min}(p) = \begin{cases} \| \mathbf{h}_{1p}^\theta \| & \text{if } 0 < p \le k_6 \\ \| 3\mathbf{h}_{1p}^\theta - \mathbf{h}_{2\bar{p}}^\theta \| & \text{if } k_6 < p \le k_7 \\ \| 2\mathbf{h}_{1p}^\theta - \mathbf{h}_{2\bar{p}}^\theta \| & \text{if } k_7 < p \le k_5 \\ \| \mathbf{h}_{1p}^\theta - \mathbf{h}_{2\bar{p}}^\theta \| & \text{if } k_5 < p \le k_1 \end{cases}$$

where k_6 and k_7 are obtained as $\| \mathbf{h}_{1p}^\theta \| = \| 3\mathbf{h}_{1p}^\theta - \mathbf{h}_{2\bar{p}}^\theta \|$ for k_6 and $\| 3\mathbf{h}_{1p}^\theta - \mathbf{h}_{2\bar{p}}^\theta \| = \| 2\mathbf{h}_{1p}^\theta - \mathbf{h}_{2\bar{p}}^\theta \|$ for k_7. Between two solutions for the equation $\| \mathbf{h}_{1p}^\theta \| = \| 3\mathbf{h}_{1p}^\theta - \mathbf{h}_{2\bar{p}}^\theta \|$, it can be shown that the smaller one is k_6

Similar to the case of $19.47^\circ \le \theta_c < 30^\circ$, p_{opt} is either k_6, k_7, k_5 or k_1, where k_6 and k_7 can be calculated from case 4 and case 3 of the Appendix, respectively. The condition on k_6 and k_7 is presented in Table 1.

Table 1 depicts the conditions to choose the optimum power loading parameters k_i for $\| \mathbf{h}_1^\theta \| \le \| \mathbf{h}_2^\theta \|$. For the case of $\| \mathbf{h}_1^\theta \| > \| \mathbf{h}_2^\theta \|$, we obtain k_i by swapping $\| \mathbf{h}_1^\theta \|$ and $\| \mathbf{h}_2^\theta \|$. Then p_{opt} is computed as $\sqrt{2 - k_i^2}$. Note that k_3 is omitted in the table, since k_3 is available only when $\| \mathbf{h}_1^\theta \| > \| \mathbf{h}_2^\theta \|$. Also Table 1 depicts the closed form expression of k_i.

Ⅳ. Simulation Results

In this section, we provide simulation results to demonstrate the effectiveness of the proposed power loading for OSM systems, and compare with the conventional OSM systems without power loading.

In Fig. 4, we compare the bit-error-rate (BER) performance of various systems. For our Monte Carlo simulations, we assume that the elements of the MIMO channel matrix $\overline{\mathbf{H}}$ are obtained from an i.i.d. complex Gaussian distribution with mean 0 and variance 1. For both QPSK and 16-QAM constellations presented in Fig. 4, we can see that our power loading algorithm provides a 5dB gain at a BER of 10^{-4} over that of no power loading case. It should be noted that our power loading method needs one additional feedback value p_{opt}. In order to demonstrate the optimality of the presented power loading, the exhaustive search result is also plotted. Out of 1000 possible power loading parameters $p \in [0, \sqrt{2}]$, the best one

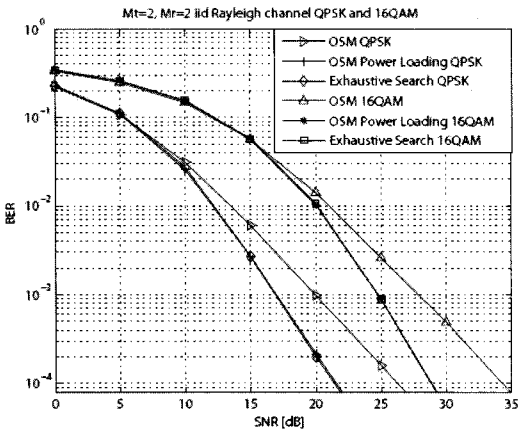

그림 4. QPSK와 16QAM에서 비트에러율
Fig. 4. BER performance of the spatial multiplexing schemes with QPSK and 16-QAM

which maximizes $d_{\min}$, is applied to the exhaustive simulation result. The best one means that it maximizes $d_{\min}$. Comparing the exhaustive search result with the proposed algorithm, we confirm that the power loading is optimal in terms of $d_{\min}$.

V. Conclusion

In this paper, we have presented a power loading algorithm for the OSM scheme in MIMO systems, which gives a good performance improvement with one additional real value for feedback information. Because of the feature of OSM systems, our algorithm performs componentwise power loading as opposed to symbolwise allocation. To determine the power loading parameter, we have illustrated a geometric approach on the minimum Euclidean distance between the constellation points in the effective channel in OSM systems. Our algorithm maximizes the minimum Euclidean distance to enhance the system performance. The simulation results confirm that the proposed algorithm for OSM is quite effective and is optimal in terms of $d_{\min}$. It is straightforward to extend the proposed algorithm to higher level modulations.

Appendix

In this Appendix, we compute p which satisfies $\| a\mathbf{h}_{1p}^{\theta}+b\mathbf{h}_{2\bar{p}}^{\theta}\|^2=\| c\mathbf{h}_{1p}^{\theta}+d\mathbf{h}_{2\bar{p}}^{\theta}\|^2$, where a, b, c and d denote integer numbers. We start with the following equation

$$\| ap\mathbf{h}_1^{\theta}+b\bar{p}\mathbf{h}_2^{\theta}\|^2=\| cp\mathbf{h}_1^{\theta}+d\bar{p}\mathbf{h}_2^{\theta}\|^2$$

It follows that

$$\begin{aligned}p^2\left(a^2\|\mathbf{h}_1^{\theta}\|^2-c^2\|\mathbf{h}_1^{\theta}\|^2-b^2\|\mathbf{h}_2^{\theta}\|^2+d^2\|\mathbf{h}_2^{\theta}\|^2\right)&\\+2(b^2-d^2)\|\mathbf{h}_2^{\theta}\|^2&\\=2p\sqrt{2-p^2}\,\|\mathbf{h}_1^{\theta}\|\,\|\mathbf{h}_2^{\theta}\|\cos\theta_c(cd-ab).&\end{aligned}$$

For the solution of the above equation, we consider the following 4 cases.

case 1 : $a=1,b=0,c=0,d=1$

$$p=\sqrt{\frac{2\|\mathbf{h}_2^{\theta}\|^2}{\|\mathbf{h}_1^{\theta}\|^2+\|\mathbf{h}_2^{\theta}\|^2}}$$

case 2 : $|a|=|c|$

$$p=\sqrt{\frac{2(b^2+d^2)\|\mathbf{h}_2^{\theta}\|^2}{4\|\mathbf{h}_1^{\theta}\|^2a^2\cos^2\theta_c+(b^2+d^2)\|\mathbf{h}_2^{\theta}\|^2}}$$

case 3 : $|b|=|d|$

$$p=\sqrt{\frac{8b^2\|\mathbf{h}_2^{\theta}\|^2\cos^2\theta_c}{(a+c)^2\|\mathbf{h}_1^{\theta}\|^2+4b^2\|\mathbf{h}_2^{\theta}\|^2\cos^2\theta_c}}$$

case 4 : $|a|\neq|c|,|b|\neq|d|$

$$p=\sqrt{\frac{-B-\sqrt{B^2-AC}}{A}}$$

where $A=(a^2-c^2)^2\|\mathbf{h}_1^{\theta}\|^4+(b^2-d^2)^2\|\mathbf{h}_2^{\theta}\|^4$
$-2(a^2-c^2)(b^2-d^2)\|\mathbf{h}_1^2\|\,\|\mathbf{h}_2^2\|+4\|\mathbf{h}_1^2\|\,\|\mathbf{h}_2^2\|$
$\times\cos^2\theta_c(cd-ab)^2$, $B=(2a^2\|\mathbf{h}_1^{\theta}\|^2-2c^2\|\mathbf{h}_1^{\theta}\|^2$
$-2b^2\|\mathbf{h}_2^{\theta}\|^2+2d^2\|\mathbf{h}_2^{\theta}\|^2)(b^2-d^2)\|\mathbf{h}_2^{\theta}\|^2-4\|\mathbf{h}_1^{\theta}\|^2$

표 2. p_{opt}의 계산값
Table 2. The Closed Form Expression of p_{opt}

k_1	$\sqrt{\frac{B}{A}}$	$A=\|\mathbf{h}_1^\theta\|^2+\|\mathbf{h}_2^\theta\|^2$ $B=2\|\mathbf{h}_2^\theta\|^2$
k_2	$\sqrt{\frac{B}{A}}$	$A=4\|\mathbf{h}_1^\theta\|^2\cos^2\theta_c+\|\mathbf{h}_2^\theta\|^2$ $B=2\|\mathbf{h}_2^\theta\|^2$
k_4	$\sqrt{\frac{-B+\sqrt{B^2-AC}}{A}}$	$A=9\|\mathbf{h}_1^\theta\|^4+\|\mathbf{h}_2^\theta\|^4-6\|\mathbf{h}_1^\theta\|^2\|\mathbf{h}_2^\theta\|^2$ $+16\|\mathbf{h}_1^\theta\|^2\|\mathbf{h}_2^\theta\|^2\cos^2\theta_c$ $B=6\|\mathbf{h}_1^\theta\|^2\|\mathbf{h}_2^\theta\|^2-2\|\mathbf{h}_2^\theta\|^4$ $-16\|\mathbf{h}_1^\theta\|^2\|\mathbf{h}_2^\theta\|^2\cos^2\theta_c$ $C=4\|\mathbf{h}_2^\theta\|^4$
k_5	$\sqrt{\frac{B}{A}}$	$A=9\|\mathbf{h}_1^\theta\|^2+4\|\mathbf{h}_2^\theta\|^2\cos^2\theta_c$ $B=8\|\mathbf{h}_2^\theta\|^2\cos^2\theta_c$
k_6	$\sqrt{\frac{-B+\sqrt{B^2-AC}}{A}}$	$A=64\|\mathbf{h}_1^\theta\|^4+\|\mathbf{h}_2^\theta\|^4-16\|\mathbf{h}_1^\theta\|^2\|\mathbf{h}_2^\theta\|^2$ $+36\|\mathbf{h}_1^\theta\|^2\|\mathbf{h}_2^\theta\|^2\cos^2\theta_c$ $B=16\|\mathbf{h}_1^\theta\|^2\|\mathbf{h}_2^\theta\|^2-2\|\mathbf{h}_2^\theta\|^4$ $-36\|\mathbf{h}_1^\theta\|^2\|\mathbf{h}_2^\theta\|^2\cos^2\theta_c$ $C=4\|\mathbf{h}_2^\theta\|^4$
k_7	$\sqrt{\frac{B}{A}}$	$A=25\|\mathbf{h}_1^\theta\|^2+4\|\mathbf{h}_2^\theta\|^2\cos^2\theta_c$ $B=8\|\mathbf{h}_2^\theta\|^2\cos^2\theta_c$

$\times \|\mathbf{h}_2^\theta\|^2\cos^2\theta_c(cd-ab)^2$ and $C=4(b^2-d^2)^2 \times \|\mathbf{h}_2^\theta\|^4$. Another solution $\sqrt{\frac{-B+\sqrt{B^2-AC}}{A}}$ is neglected, since this solution is larger than the other one.

References

[1] A. J. Paulraj, D. A. Gore, R. U. Nabar, and H. Bolcskei, "An overview of MIMO communications-A key to gigabit wireless," in *Proc. IEEE*, vol. 92, pp. 198-218, February 2004.

[2] G. J. Foschini and M. Gans, "On Limits of Wireless Communications in a Fading Environment when Using Multiple Antennas," *Wireless Personal Communications*, vol. 6, pp. 311-335, March 1998.

[3] I. E. Telatar, "Capacity of multi-antenna Gaussian channels," *Eur. Trans. Telecom,* vol. 10, pp. 585-595, November 1999.

[4] S. M. Alamouti, "A simple transmit diversity techniques for wireless communications," *IEEE Journal on Selected Areas in Communications*, vol. 16, pp. 1451-1458, October 1998.

[5] V. Tarokh, N. Seshadri, and A. R. Calderbank, "Space-time codes for high data rate wireless communication : performance criterion and code construction," *IEEE Transactions on Information Theory*, vol. IT-44, pp. 744-765, March 1998.

[6] V. Tarokh, H. Jafarkhani, and A. R. Calderbank, "Space-time block codes from orthogonal designs," *IEEE Transactions on Information Theory*, vol. 45, pp. 1456-1467, July 1999.

[7] G. J. Foschini, "Layered space-time architecture for wireless communication in a fading environment when using multi-element antennas," *Bell Labs. Tech. J.*, vol. 1, pp. 41-59, 1996.

[8] G. J. Foschini, G. D. Golden, R. A. Valenzuela, and P. W. Wolniansky, "Simplified Processing for High Spectral Efficiency Wireless Communication Employing Multi-Element Arrays," *IEEE Journal on Selected Areas in Communications*, vol. 17, pp. 1841-1852, November 1999.

[9] G. J. Foschini, D. Chizhik, M. J. Gans, C. apadias, and R. A. Valenzuela, "Analysis and Performance of Some Basic Space-Time Architectures," *IEEE Journal on Selected Areas in Communications*, vol. 21, pp. 303-320, April 2003.

[10] G. G. Raleigh and J. M. Cioffi, "Spatio-Temporal Coding for Wireless Communication," *IEEE Transactions on Communications*, vol. 46, pp. 357-366, March 1998.

[11] H. Sampath, P. Stoica, and A. Paulraj, "Generalized Linear Precoder and Decoder Design for MIMO Channels Using the Weighted MMSE Criterion," *IEEE Transactions on Communications*, vol. 49, pp. 2198-2206, December 2001.

[12] G. H. Golub and C. F. V. Loan, *Matrix Computations*. Second Edition, The Johns Hopkins University Press, Baltimore and London, 1989.

[13] A. Narula, M. J. Lopez, M. D. Trott, and G. W. Wornell, "Efficient Use of Side Information

in Multiple-Antenna Data Transmission over Fading Channels," *IEEE Journal on Selected Areas in Communications*, vol. 16, pp. 1423-1436, October 1998.

[14] D. J. Love and R. W. Heath, "Limited Feedback Unitary Precoding for Spatial Multiplexing Systems," *IEEE Transactions on Information theory*, vol. 51, pp. 2967-2976, August 2005.

[15] H. Lee, S. Park, and I. Lee, "Orthogonalized Spatial Multiplexing for MIMO systems," *IEEE Transactions on Communications*, April 2007.

[16] H. Lee, S. Park, and I. Lee, "Orthogonalized Spatial Multiplexing for MIMO systems," in *Proc. VTC*, September 2006.

[17] R. W. Heath and A. J. Paulraj, "Antenna Selection for Spatial Multiplexing Systems based on minimum error rate," *Proc. of ICC*, vol. 7, pp. 2276-2280, June 2001.

김 영 태 (Young-Tae Kim) 정회원

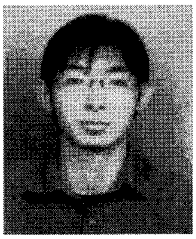

2006년 2월 고려대학교 전기전자전파공학부 졸업

2008년 2월 고려대학교 전자전기공학과 석사

2008년 3월~현재 고려대학교 전자전기공학과 박사과정

<관심분야> Signal processing and coding theory for wireless communication, information theory

박 석 환 (Seokhwan Park) 정회원

2005년 2월 고려대학교 전기전자전파공학부 졸업

2007년 2월 고려대학교 전자전기공학과 석사

2007년 3월~현재 고려대학교 전자전기공학과 박사과정

<관심분야> Signal processing and coding theory for wireless communication, information theory

이 인 규 (Inkyu Lee) 종신회원

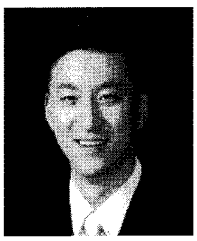

1990년 2월 서울대학교 제어계측공학과 졸업

1992년 2월 스탠포드대학교 전자공학과 석사

1995년 2월~현재 스탠포드대학교 전자공학과 박사

2002년 9월~현재 고려대학교 전기전자전파공학부 정교수

<관심분야> Digital communication, signal processing and coding technique applied to wireless communication